

Article

Pullulan Films with PCMs: Recyclable Bio-Based Films with Thermal Management Functionality

Nuray Kizildag

Institute of Nanotechnology, Gebze Technical University, Gebze 41400, Kocaeli, Turkey; nuraykizildag@gtu.edu.tr

Abstract: The use of phase-changing materials (PCMs) is a practical and powerful way of buffering thermal fluctuations and maintaining the isothermal nature of the storage process. In this study, melamine formaldehyde microcapsules with paraffin cores were used as PCMs; pullulan films with PCMs were prepared by the film-casting method; and the composite films prepared were analysed with regard to their chemical structure, thermal properties, thermal stability, and recyclability. Uniform films displaying thermal management functionality were prepared. The amount of 75 wt.% PCM were added to the pullulan film structure which enabled the preparation of a composite film that displayed 104.85 J g^{-1} of heat storage during heating and 103.58 J g^{-1} of heat release during cooling. Multiple heating and cooling cycles showed that the composite films maintained their thermal management functionality after multiple heating-cooling cycles. The PCMs could be recovered with a yield of approximately 95% by the application of a simple dissolution and filtration process. The morphology, chemical structure, and thermal properties of the PCMs were maintained after the recovery process. The bio-based composite films with thermal management functionality and recyclability are proposed as an innovative, practical, and effective system for thermoactive storage and packaging applications.

Keywords: bio-based; encapsulated PCMs; packaging films; phase-changing materials; pullulan; recyclable; thermal management; thermoactive; thermoregulation



Citation: Kizildag, N. Pullulan Films with PCMs: Recyclable Bio-Based Films with Thermal Management Functionality. *Coatings* **2023**, *13*, 414. <https://doi.org/10.3390/coatings13020414>

Academic Editor: Ivan Jerman

Received: 1 January 2023

Revised: 30 January 2023

Accepted: 10 February 2023

Published: 12 February 2023



Copyright: © 2023 by the author. Licensee MDPI, Basel, Switzerland. This article is an open access article distributed under the terms and conditions of the Creative Commons Attribution (CC BY) license (<https://creativecommons.org/licenses/by/4.0/>).

1. Introduction

Packaging materials produced by using non-biodegradable synthetic polymers cause significant environmental problems. Bio-based polymers have drawn great attention in the last decade due to rising environmental concerns about the inappropriate disposal of plastics, the limitations of petroleum-based polymers, and the high price of oil. As a result, the focus of research has shifted to the development of eco-friendly and sustainable packaging materials [1–4]. Pullulan is an exopolysaccharide obtained from the yeast-like fungus *Aureobasidium* for commercial use. Because of the low degree of hydrogen bonding in its crystal form, it is easily water-soluble. As a water-soluble and non-toxic biopolymer with superior film-forming and adhesive properties, it offers great potential to produce films and coatings for packaging applications. Solvent casting, extrusion, coating, layer-by-layer assembly, and electrospinning are the main methods used to fabricate pullulan-based films/coatings. Aqueous solutions with pullulan concentrations of 2%–20% make it possible to prepare films and coatings by dipping, spraying, or brushing. Pullulan has a wide range of applications in many fields such as food storage, health care, pharmacy, medical, biomedical, and even lithography [1].

The addition of functional additives into the polymer matrix enables the production of nano/microcomposites with distinguishing functional properties. An increasing number of publications on the modification of pullulan with different types of additives are seen. Nanofibrillated cellulose [5], microfibrillated cellulose [6], lysozyme [7], montmorillonite [8,9], nanoSiO₂ [2], nanosilver [10], and TiO₂ [11] have been used to improve either structural or functional properties of pullulan films.

Depending on the medium temperature, PCMs are able to absorb, store, and release large amounts of latent heat due to their phase transition properties [12–16]. PCMs are categorized into three groups: organic, inorganic, and eutectics of the first two. Paraffin waxes, polyethylene glycols (PEGs), and fatty acids are organic PCMs, whereas metals, metal alloys, salts, and salt hydrates are inorganic PCMs. The melting temperature, temperature range of the phase-change, and heat storage capacity are important properties of the PCMs that determine the selection of the PCMs for a particular end use [16]. Leakage of PCM materials when they are in a melt state is a common problem with PCMs. They are usually not embedded into the structure of polymeric materials but are first encapsulated and then applied in the form of microencapsulated PCMs (microPCMs). Microencapsulation is an effective method to prevent the leakage of the PCMs and their reaction to the outside environment. Microcapsules are produced by coating a thin and resilient polymer onto small solid particles or liquid droplets [16–19]. The microencapsulation of PCMs results in some useful effects for heat storage, such as tailorable shape, favourable temperature gradient, and increased lifetime. Furthermore, the PCMs are always in a dried state as the phase change takes place within the coating layer. Microencapsulation increases the specific exchange area, which aids in effective heat transfer and avoids problems such as supercooling and phase separation. The walls protect the core materials from their environment prior to use, provide safe and convenient handling of core materials, and result in increased heat resistance [16].

Organic PCMs are used to produce novel materials with thermal management functionality for many different applications such as smart textiles [20], construction [21,22], photocatalytic applications [23], photovoltaic systems [24], biomedical applications [25], electrics and electronics [26], and packaging materials [27]. Recently, many novel approaches have appeared in the literature for the development of materials with thermal management properties. For example, researchers developed fibrous wearable strain sensors by decorating plant-extracted 3D porous *Juncus effusus* fibers with conductive graphene/polypyrrole which also showed electric-thermal properties. The fibers showed fast heating properties with the application of voltage. It could be possible to achieve a temperature of 147 °C at 10 V within 10 s [28]. In another study, a fiber membrane was fabricated using poly (vinylidene fluoride-co-hexafluoro propene) and polypyrrole. The membrane displayed multifunctional properties of radiative cooling and solar heating for efficient daytime outdoor thermal management. The multifunctional membrane presented a sun-ambient cooling temperature of ~4.5 °C and a super-ambient heating temperature of ~35.8 °C in an outdoor environment under the solar intensity of ~850 W m⁻² [29]. The nanoprocessing of silk through a molecular bonding design and scalable coupling reagent-assisted method achieved sub-ambient daytime radiative cooling. In simulation studies, the temperature of skin covered with nanoprocessed silk showed a temperature 8 °C lower than skin covered with natural silk and cotton. The nanoprocessed silk fabric was durable even through water washing and sunlight drying. The study provided a sustainable, energy-saving method for personal thermal management and contributed to the field of green energy [30]. Other than the novel approaches to developing materials with thermal management properties, great effort is being invested in developing recyclable materials following the concept of “design for recycling”. In this study, pullulan-based, recyclable composite films with thermal management functionality were prepared with the incorporation of PCMs as alternative thermoactive packaging materials. Although many studies investigate and report the properties of PCMs and composite materials (coatings, films, fibers, and nanofibers) with PCMs, a very limited number of studies show the preparation of bio-based, easily recyclable films with thermal management properties. Pullulan is specifically chosen as a bio-based, water-soluble polymer that enables the easy application of its solutions by immersion, spraying, or brushing. Nextek 28D PCMs, which are microcapsules of melamine formaldehyde containing paraffin, were selected as shape-stable phase-changing materials and incorporated into pullulan films. The morphology, chemical structure, thermal properties, stability, and recyclability of biomicrocomposite

films were analysed in detail. This study offers significant contribution to the efforts to “design for recycling” and the literature by showing the development of eco-friendly and recyclable thermoactive films which are chemically, morphologically, and thermally stable.

2. Experimental details

2.1. Materials

Food-grade pullulan with a molecular weight of 100 kDa was kindly provided by Hayashibara Biochemical Laboratories, Inc., and used for the preparation of neat and composite films. Pullulan polymer was dissolved in distilled water for film preparation. Nextek 28D phase-changing microcapsules with a peak melting point of 28 °C were kindly provided by Microtek Laboratories, Inc. (Moraine, OH, USA), and incorporated into the pullulan film structure to obtain biomicrocomposite films showing thermal management functionality. The properties of the Nextek 28D microcapsules are presented in Table 1. Ethyl acetate was used as the nonsolvent for the precipitation of pullulan during the recovery of pullulan in powder form.

Table 1. Properties of Nextek 28D microcapsules.

Properties	Nextek 28D
Appearance	White to slightly off-white color
Form	Dry powder (>97 solids)
Particle size (mean)	15–30 micron
Free wax content	<2.5%
Melting point	28 °C (± 2 °C)
Heat of fusion	>155 J/g

2.2. Methods

2.2.1. Preparation of the Solutions

Distilled water was used as the solvent for dissolving pullulan. Certain amounts of PCMs added into certain amounts of distilled water were homogenized in an ultrasonic bath at room temperature for 30 min. Then pullulan was added and magnetically stirred at room temperature for 2 h until complete dissolution. The concentration of pullulan was 10 wt.% in the composite solutions. Reference films were also cast from 10 wt.% pullulan/distilled water solution. The photographs of the pullulan solution and composite pullulan solution containing 75 wt.% PCMs are presented in Figure 1.

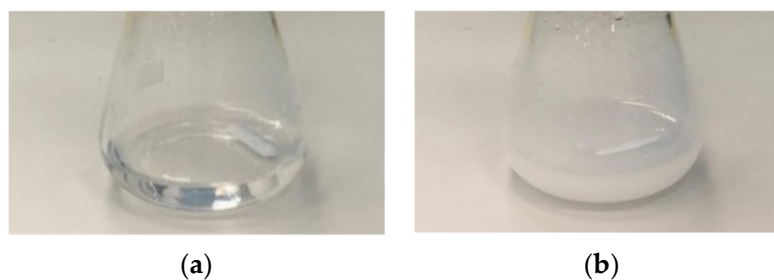


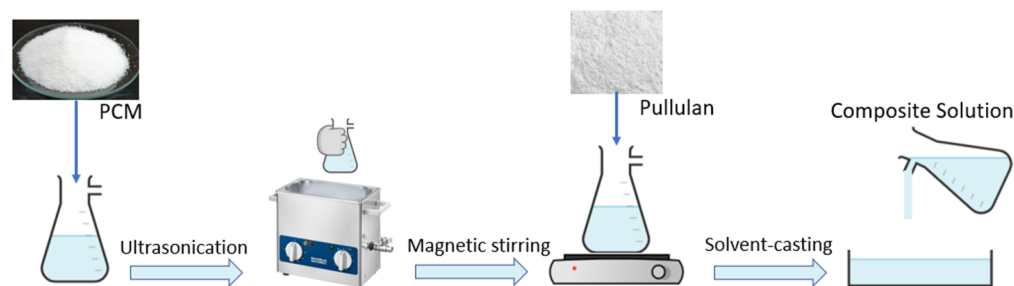
Figure 1. Photographs of (a) pullulan solution and (b) composite solution.

2.2.2. Film Preparation

The amount of 20 mL of composite solutions containing different amounts of PCMs was cast on a petri dish and left at room temperature for drying. The PCM contents in the composite films based on film weight are presented in Table 2. The wt.% of PCMs based on the film weight can be seen in the table. “P” is used to denominate Pullulan, and “NEX” is used to denominate the phase change material, NEXTEK 28D. The schematic diagram showing the preparation of pullulan-based thermoactive films is presented in Figure 2.

Table 2. Formulations of the pullulan-based thermoactive films.

Samples	PCM Content (wt.%) (Based on Film Weight)
P	-
P-NEX15	15
P-NEX30	30
P-NEX45	45
P-NEX60	60
P-NEX75	75

**Figure 2.** Schematic diagram showing the preparation of the pullulan-based composite films.

2.2.3. Recycling Process Applied for the Recovery of Pullulan and PCMs

Distilled water was used to dissolve the P-NEX75 film (composite film containing 75 wt.% PCMs), and the solution was filtered through a standard laboratory filter paper for the recovery of the PCM particles and the polymer pullulan. After the filtration, the solution was added to ethyl acetate for the precipitation of pullulan in powder form. The recovered pullulan powder was analysed by FTIR to confirm that it did not contain any PCMs. The recovered PCM microcapsules were tested with regard to their morphology and thermal performance in order to ensure that they were reusable.

2.3. Characterization

2.3.1. Fourier Transform Infrared Spectrometer (FTIR)

FTIR (Perkin Elmer-Spectrum Two) with an ATR accessory was employed to record absorption spectra of pullulan polymer, encapsulated PCMs, and composite films in a range from 4000 to 600 cm^{-1} with a resolution of 4 cm^{-1} . FTIR spectra of the samples were obtained by averaging 32 scans taken for each sample. The chemical structure of recovered pullulan and encapsulated PCMs were also analysed using FTIR spectroscopy.

2.3.2. Differential Scanning Calorimetry (DSC)

Mettler Toledo (Columbus, OH, USA) was used to investigate the thermal properties of pullulan, encapsulated PCMs, and composite films prepared. The latent heat storage and release ability of the materials were evaluated by testing in a temperature range from 0 $^{\circ}\text{C}$ to 50 $^{\circ}\text{C}$, with a heating/cooling rate of 5 $^{\circ}\text{C min}^{-1}$, under nitrogen (N_2) with a flow rate of 20 mL min^{-1} . All samples were brought to thermal equilibrium at the starting temperature, held for 10 min, then heated to the final temperature of a 5 $^{\circ}\text{C min}^{-1}$ heating rate where they were held for 10 min. The thermal characteristics were evaluated from the second heating of the samples. The peak points of the phase transition regions were taken as the phase transition temperature. The areas under the solid–liquid and liquid–solid phase change peaks were calculated to determine the melting enthalpy (ΔH_m) and crystallization enthalpy (ΔH_c), respectively. DSC was also utilized to confirm the thermal stability of the recovered PCMs following the same testing procedure.

2.3.3. Thermal Stability

Fifty consecutive heating-cooling cycles between 0 and 50 °C with a heating rate of 5 °C min⁻¹ were applied to the composite film containing 75 wt.% PCMs to evaluate the changes in the latent heat storage and release ability of the composite film by repeated thermal cycles. The process also was used to confirm the thermal stability of the pullulan-based thermoactive films. The phase transition temperature was taken as the peak point of the DSC curves. The areas under the solid-liquid and liquid-solid phase change peaks were calculated to determine the ΔH_m and ΔH_c , respectively.

2.3.4. Optical Microscope (OM)

An Olympus BX51 optical microscope manufactured by Olympus Corporation (Tokyo, Japan) was used to confirm the form stability of PCM microcapsules after the recovery process.

3. Results and Discussion

3.1. Pullulan-Based Thermoactive Films

3.1.1. Appearance of the Films Prepared

Photographs of neat pullulan and composite pullulan films containing 75 wt.% encapsulated PCMs are presented in Figure 3. Both films were smooth. The composite films turned to a white colour with the addition of the microcapsules.

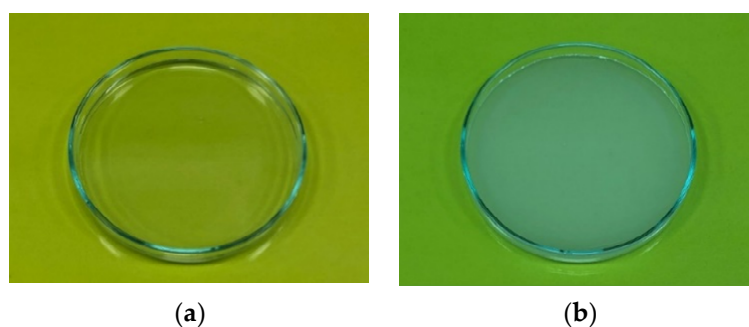


Figure 3. Photographs of (a) neat pullulan film and (b) composite film with 75 wt.% PCMs.

3.1.2. Fourier Transform Infrared Spectroscopy (FTIR)

FTIR spectroscopy was used to confirm the incorporation of PCM into the pullulan film structure. Additionally, the spectra were used to compare the differences between the chemical structure of composite films and the neat pullulan films. The normalized FTIR spectra of PCMs (Nextek 28D) and pullulan powder used in the preparation of the films are presented in Figure 4, while the FTIR spectra of the composite films are presented in Figure 5.

The composite films were expected to display absorbance signals corresponding to the molecular structure of pullulan, crosslinked melamine formaldehyde, and paraffin. Pullulan is a linear homopolysaccharide, the building block of which is a maltotriose. Maltotriose units are bonded to each other by α -(1,6) bonds and three glucose units of maltotriose are bonded through α -(1,4) glycosidic bonds to another three glucose units of maltotriose to form the pullulan repeating unit. For pullulan, a broad peak located at around 3330 cm⁻¹ was assigned to -OH stretching vibrations which is extensively observed in the polysaccharide structures. The peak around 2924 cm⁻¹ corresponded to the C-H vibrations of methyl groups, including CH₂ and CH₃ [31–33]. In addition, only a single peak at 1642 cm⁻¹ was assigned to the stretching vibration of O-C-O in pullulan. Other features of pullulan were also observed in the spectra, including C-OH bend (1354 cm⁻¹) and C-O-C stretch (1148 cm⁻¹). The peaks at 1076 and 1020 cm⁻¹ were attributed to the vibration of C-O-H and C-O bands, respectively. The typical absorption bands for the α -configuration of α -D-glucopyranoside units in pullulan were observed at 851 cm⁻¹. In addition, the two main linkages of pullulan (i.e., α -(1,4) and α -(1,6)-D-glycosidic bonds) were observed at 738 and 918 cm⁻¹ [34–40]. Nextek 28D is a PCM material that consists of a highly-crosslinked melamine formaldehyde shell containing paraffin in the core. Therefore,

peaks related to both highly-crosslinked formaldehyde and paraffin are expected to be observed in the FTIR spectrum of the PCMs. In the spectrum of Nextek 28D, the peak at 3337 cm^{-1} may be assigned to the O-H and shows the presence of moisture in the PCMs. Paraffins show bands located at 2954 , 2914 , and 2848 cm^{-1} corresponding to the characteristic peaks of the aliphatic C-H stretching vibrations. The peak at 1470 cm^{-1} was assigned to the bending vibration of the $-\text{CH}_2$ groups, and 716 cm^{-1} to the rocking vibrations of C-H in the paraffin [41]. Crosslinked melamine formaldehydes give FTIR absorbance signals at 3335 cm^{-1} , which can be assigned to the secondary amine vibrations; between 2940 and 2915 cm^{-1} to asymmetric stretching vibrations; and between 2870 and 2840 cm^{-1} to the symmetric stretching vibrations of CH_2 groups. These all overlap with those coming from the CH_2 groups of the paraffins. The peaks at 1551 cm^{-1} are attributed to the stretching of triazine rings. Peaks at 1470 cm^{-1} are expected to appear due to several C-H vibrations [42]. The band at 1157 cm^{-1} corresponds to $\text{C}_\text{R}-\text{N}$ stretching and asymmetrical C-O-C stretching vibration in $-\text{CH}_2-\text{O}-\text{CH}_2-$ group. The bands between 1360 and 1320 in MF resins are assigned to the sidegroup-sensitive $\text{C}_\text{AR}-\text{N}$ stretching vibrations, while the band at 891 cm^{-1} is assigned to the $-\text{CH}_2$ twisting vibration [42].

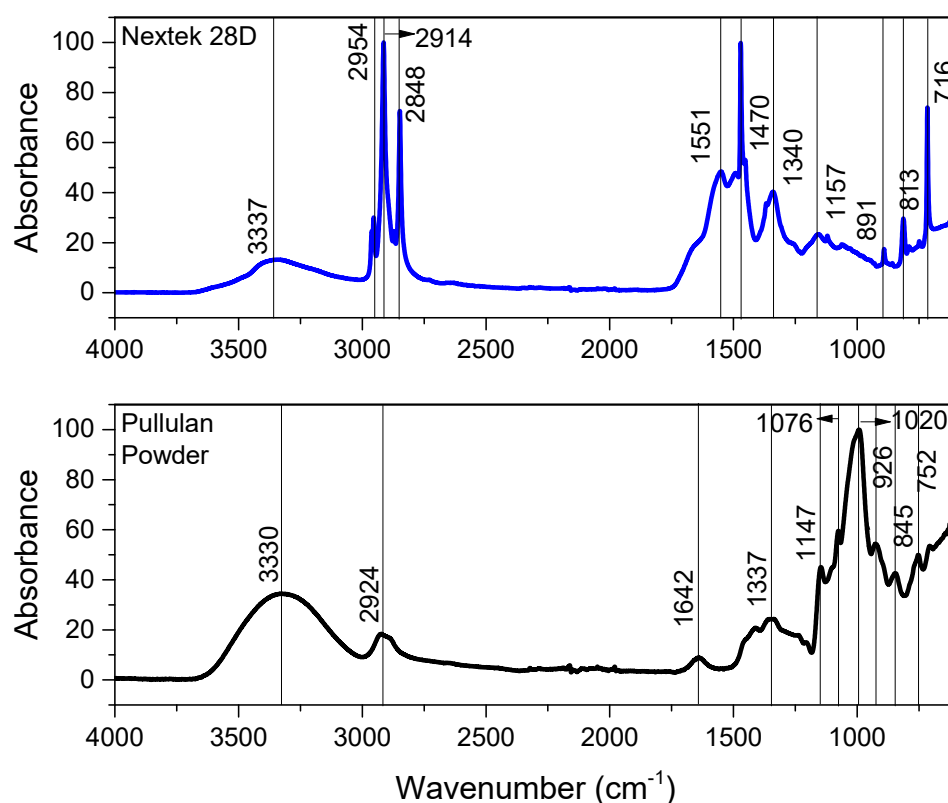


Figure 4. FTIR spectra of PCMs (Nextek 28D) and neat pullulan powder.

The spectra of composite films were normalized to the largest peak observed, namely the C-O stretchings observed at 1020 cm^{-1} , in order to be able to show the changes in the intensities of the PCM-related peaks with the changes in PCM contents. According to Figure 5, remarkable differences in spectra profiles were detected between pure pullulan films and composite films. The absorption bands observed in the spectra of the composite films were a combination of the pullulan polymer and highly crosslinked PCMs. The absorbance values of the peaks, which were related to PCMs, increased with the increase in the PCM content. Showing the typical peaks of PCMs in addition to the typical peaks of pullulan, the FTIR spectra of composite films confirmed the incorporation of PCMs into the pullulan films. As there were no significant shifts in the locations of the peaks, it was concluded that no chemical reactions occurred between pullulan polymer and PCMs.

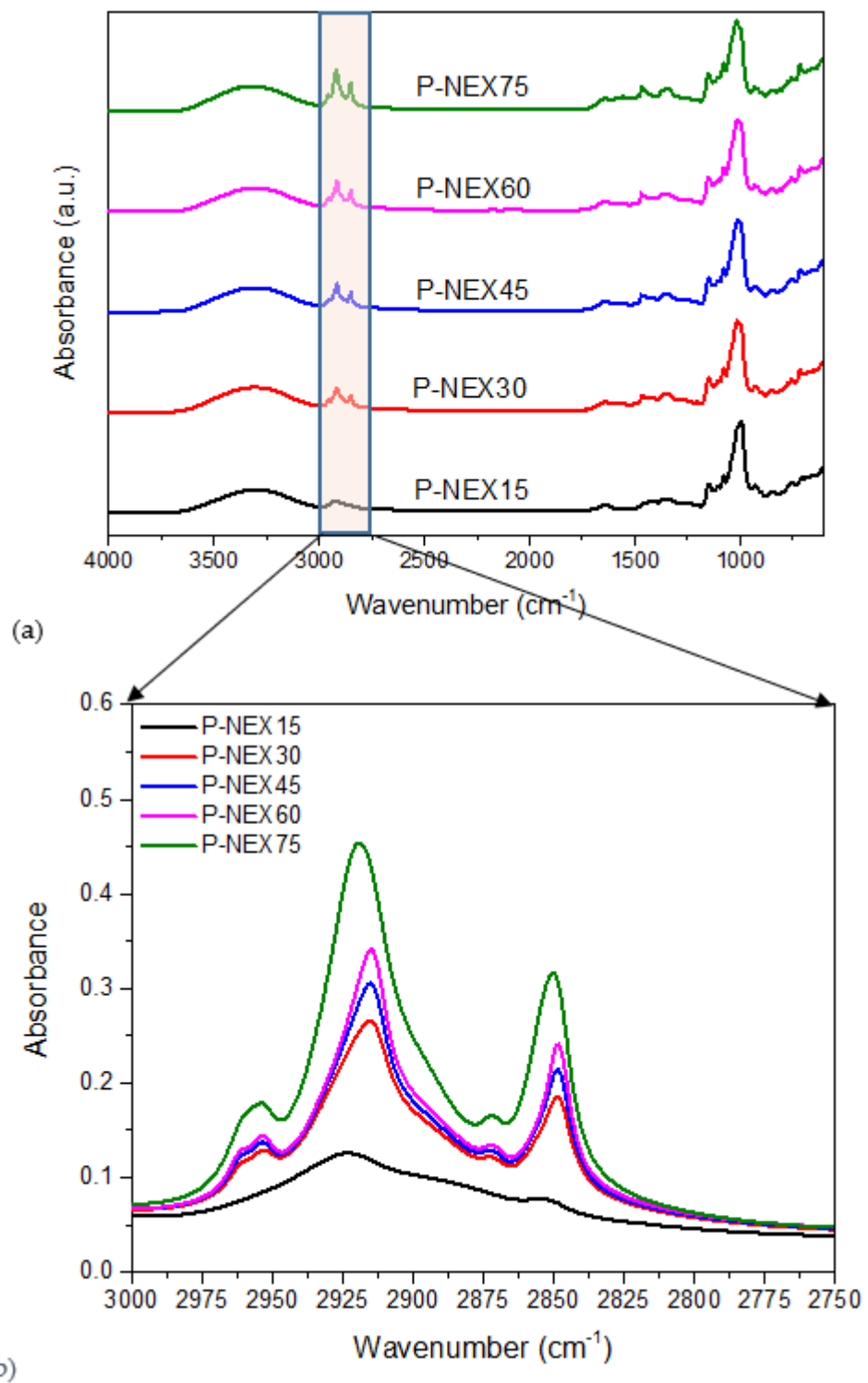


Figure 5. FTIR spectra of composite films at (a) 4000 to 600 cm^{-1} range; (b) 3000 to 2750 cm^{-1} range.

3.1.3. Thermal Management Functionality

Thermal management properties of PCM materials are effectively tested by using DSC. The amount of energy that can be stored and released by a material can be determined by applying heating and cooling cycles within a certain temperature range. The melting enthalpy shows the amount of energy that can be stored, and the crystallization enthalpy shows the energy that can be released [43]. For packaging materials with thermal management functionality, proper phase-change temperature and high latent heat storage capability is

the most important characteristic. In this study PCM material, which displayed a melting point of around 28 °C was specially chosen. The pullulan polymer, encapsulated PCMs, and pullulan-based thermoactive films containing encapsulated PCMs were characterised with regard to their thermal properties, i.e., melting temperature (T_m), melting enthalpy (ΔH_m), crystallization temperature (T_c), and crystallization enthalpy (ΔH_c) via DSC. DSC thermograms of pullulan powder and encapsulated PCMs are presented in Figure 6, while the DSC thermograms of pullulan-based films and pullulan-based thermoactive composite films are presented in Figure 7.

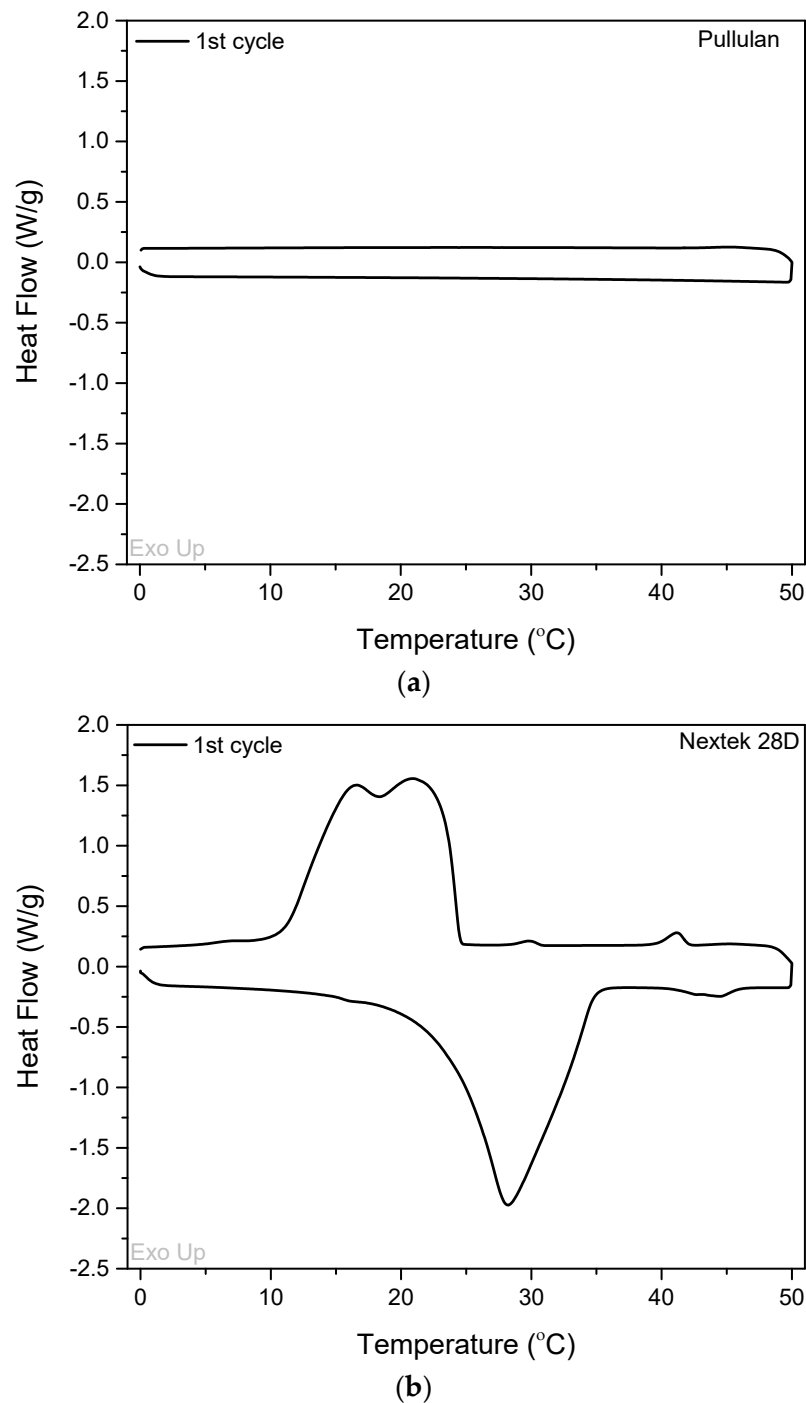


Figure 6. Three cycle heating and cooling curves of (a) Pullulan and (b) encapsulated PCMs (Nextek 28D).

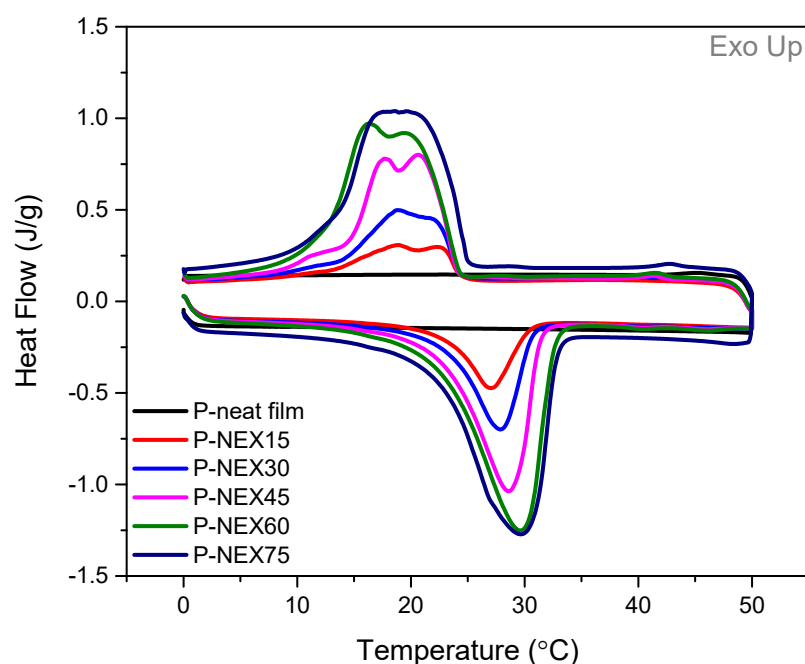


Figure 7. Heating and cooling curves of pullulan and pullulan-based thermoactive films.

While neat pullulan powder showed no phase transitions between 0 and 50 °C, encapsulated PCMs displayed a large exothermic (crystallization) peak between around 25 and 35 °C and an endothermic peak at around 28 °C. The melting and crystallization enthalpies of the encapsulated PCMs were measured as 173.26 and 170.50 J g⁻¹, respectively. Thermal properties of the pullulan-based thermoactive films were expected to be dominated by the PCM type and PCM content. The phase-change temperatures and the possible maximum value of the latent heat were to be determined by the PCM type, whereas the actual value of the latent heat was expected to be determined by the PCM content of the composite films.

According to the FTIR analysis, no interactions occurred between the polymer and the PCMs. Pullulan-based thermoactive composite films showed phase change because of the encapsulated PCMs in the film structure, and no additional effects were expected as there were no interactions between the components of the composite films. The corresponding phase transition temperatures and enthalpy values of composite films are summarized in Table 3. The phase change temperatures (T_m and T_c) of the films were dominated by the PCM properties and showed no obvious variations compared to those of the PCMs. The slight increase in the melting temperature and the crystallization temperature with the increase in the additive content was likely due to the differences in the thermal conductivity properties of the polymer and PCMs. An increase in the PCM concentration resulted in an increase in the storage and release enthalpy values. The ΔH_m increased from 21.94 to 104.85 J g⁻¹, whereas ΔH_c increased from 20.92 to 103.58 J g⁻¹ as the PCM content increased from 15 to 75 wt.%. The highest storing and releasing enthalpy values were obtained for the pullulan-based thermoactive films with the highest content of PCMs. Preparing PAN nanofibers with 50 wt.% paraffinic PCMs, Kizildag et al. reported that the composite nanofibers showed storage and release enthalpies of 58.74 J g⁻¹ and 57.41 J g⁻¹, respectively [44]. In another study, a shape-stabilized and flexible phase change film was prepared based on polyethylene glycol (PEG), which was stabilized by the cooperation of cellulose nanofibers (CNF) and expanded graphite (EG). The thermal conductivity of the prepared film was enhanced by boron nitride (BN). The results showed that the phase change enthalpy of the film could reach 79.46 J g⁻¹ and remained almost unchanged during 40 heating–cooling cycles [45]. The thermoregulation performances obtained for the pullulan-based composite films with PCMs were in parallel with the results reported in the literature.

Table 3. Thermal properties of pullulan and pullulan-based thermoactive films between 0 and 50 °C.

Samples	Melting Temp. (°C)	Latent Heat of Melting (ΔH_m) (J g ⁻¹)	Crystallization Temp. (°C)	Latent Heat of Crystallization (ΔH_c) (J g ⁻¹)
neat Pullulan	-	-	-	-
P-NEX15	27.04	21.94	18.23/22.04	20.92
P-NEX30	27.86	37.65	18.79/22.02	37.69
P-NEX45	28.50	66.54	17.96/20.73	65.41
P-NEX60	29.47	87.83	15.70/20.56	85.67
P-NEX75	29.36	104.85	16.02/18.82	103.58

The enthalpy values of pullulan-based thermoactive films were lower than that of encapsulated PCMs because the polymer (pullulan) in the composite films did not have any phase transitions in the temperature range between 5 and 50 °C. Additionally, some differences were observed in the enthalpy values measured for the composite films and theoretical enthalpy values calculated. The theoretical and experimental enthalpy values obtained by DSC are presented in Table 4. Theoretical enthalpy values of the composite films were calculated by multiplying the melting/crystallization enthalpy and mass percentage of the PCM in the composite film. From Table 4, all the experimental values of enthalpy were lower than the corresponding theoretical values, and the efficiency of enthalpy, which was calculated as the ratio of the experimental value to the theoretical values, was less than 100%. The differences between the experimental values and theoretical values were attributed to the hindrance of pullulan by acting as a diluent for the PCMs and preventing them to form well-defined structures in the composite films [44].

Table 4. Theoretical and experimental enthalpy values.

	Theoretical Value (ΔH_m) (J g ⁻¹)	Experimental Value (ΔH_m) (J g ⁻¹)	%	Theoretical Value (ΔH_c) (J g ⁻¹)	Experimental Value (ΔH_c) (J g ⁻¹)	%
P-NEX15	25.99	21.94	84.4	25.58	20.92	81.8
P-NEX30	51.98	37.65	72.4	51.15	37.69	73.7
P-NEX45	77.97	66.54	85.3	76.73	65.41	84.8
P-NEX60	104.00	87.83	84.5	102.30	85.46	83.5
P-NEX75	129.95	104.85	80.7	127.88	103.58	81.0

3.1.4. Stability Analysis—Repeated Heating & Cooling Cycles

The thermal stability of pullulan-based thermoactive film containing 75 wt.% PCMs (P-NEX75) was tested by applying 50 consecutive thermal cycles. The thermograms of the first and fiftieth cycles are presented in Figure 8a. In the inset, the thermograms of 50 cycles are presented. The changes in melting, crystallization enthalpies, and phase-change temperatures are presented in Figure 8b. The long-term stability of the pullulan-based thermoactive films was confirmed as no significant changes were observed in the phase transition temperatures and enthalpies. Additionally, the thermal cycles applied showed that no thermal evaporation (thus no PCM loss) took place during the repeated cycles. Furthermore, the application of thermal cycles indicated that the thermal properties of the composite films were almost unchanged after the test completion.

3.2. Recovery of Pullulan and PCMs

Pullulan-based thermoactive film containing 75 wt.% PCMs was dissolved in distilled water, and the solution was filtered through a standard laboratory filter paper for the recovery of the PCM particles and the polymer pullulan. After the filtration, the solution was added to ethyl acetate for the precipitation of pullulan in powder form. The recovered pullulan powder was analysed by FTIR to confirm that it did not contain any PCMs. The recovered PCM microcapsules were tested with regard to their morphology and thermal performance in order to ensure that they were reusable. The PCMs and pullulan polymer could be recovered with a yield of approximately 95% and 93% respectively. The

optical microscope images, FTIR spectra, and DSC thermograms of the recovered PCMs in comparison to the original PCMs showed that the morphology, chemical structure, and thermal properties of the recovered PCMs were maintained after the recovery process. All of these results showed that the PCMs were reusable (Figure 9a–c). The FTIR spectrum of the recovered pullulan was identical to the fresh pullulan polymer (Figure 10).

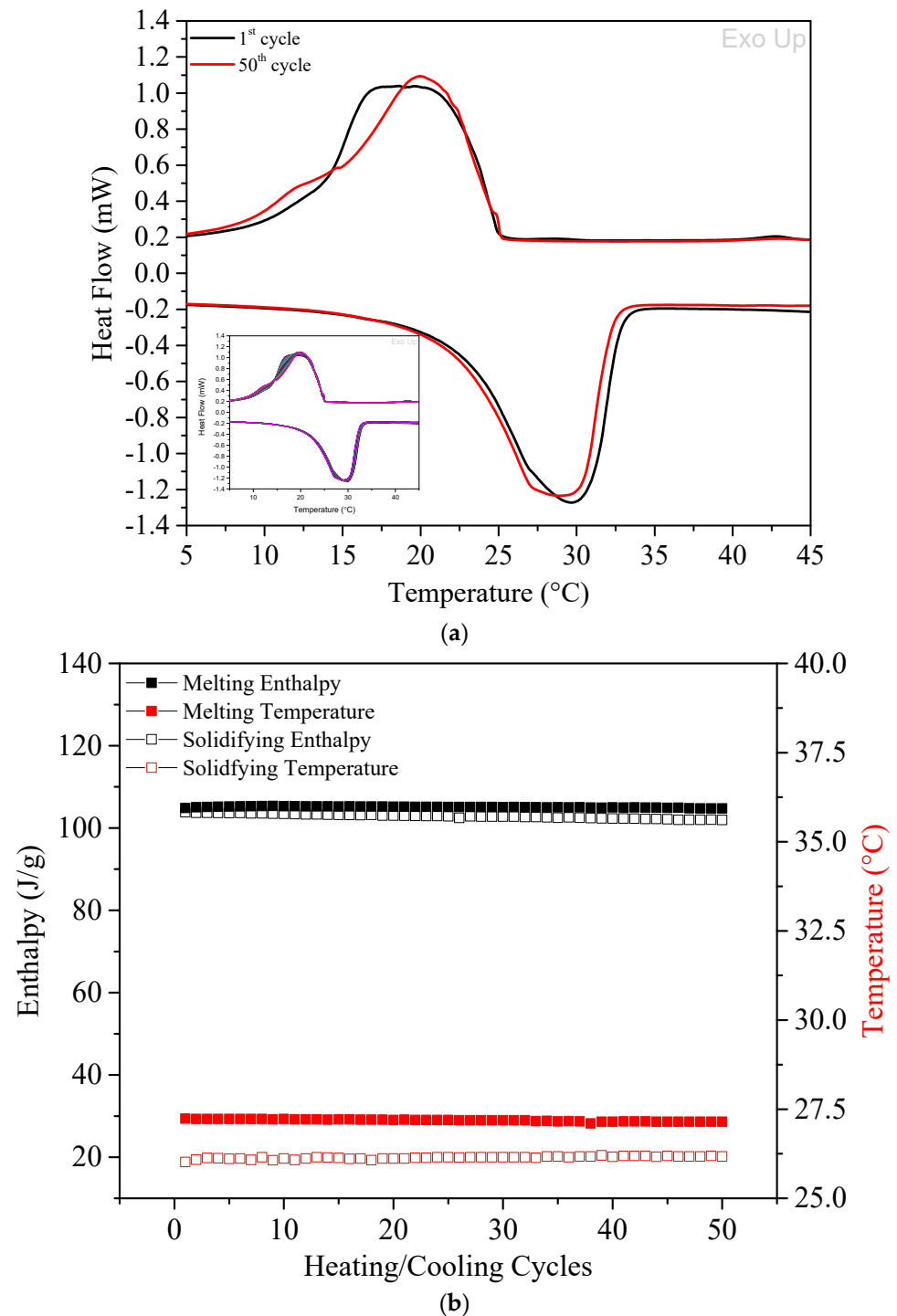


Figure 8. (a) DSC curves of 1st and 50th thermal cycles with thermograms of 50 thermal cycles presented in the inset; (b) variations in storage and release enthalpies and thermal transition temperatures during thermal cycles for composite films containing 75 wt.% PCM (P-NEX75).

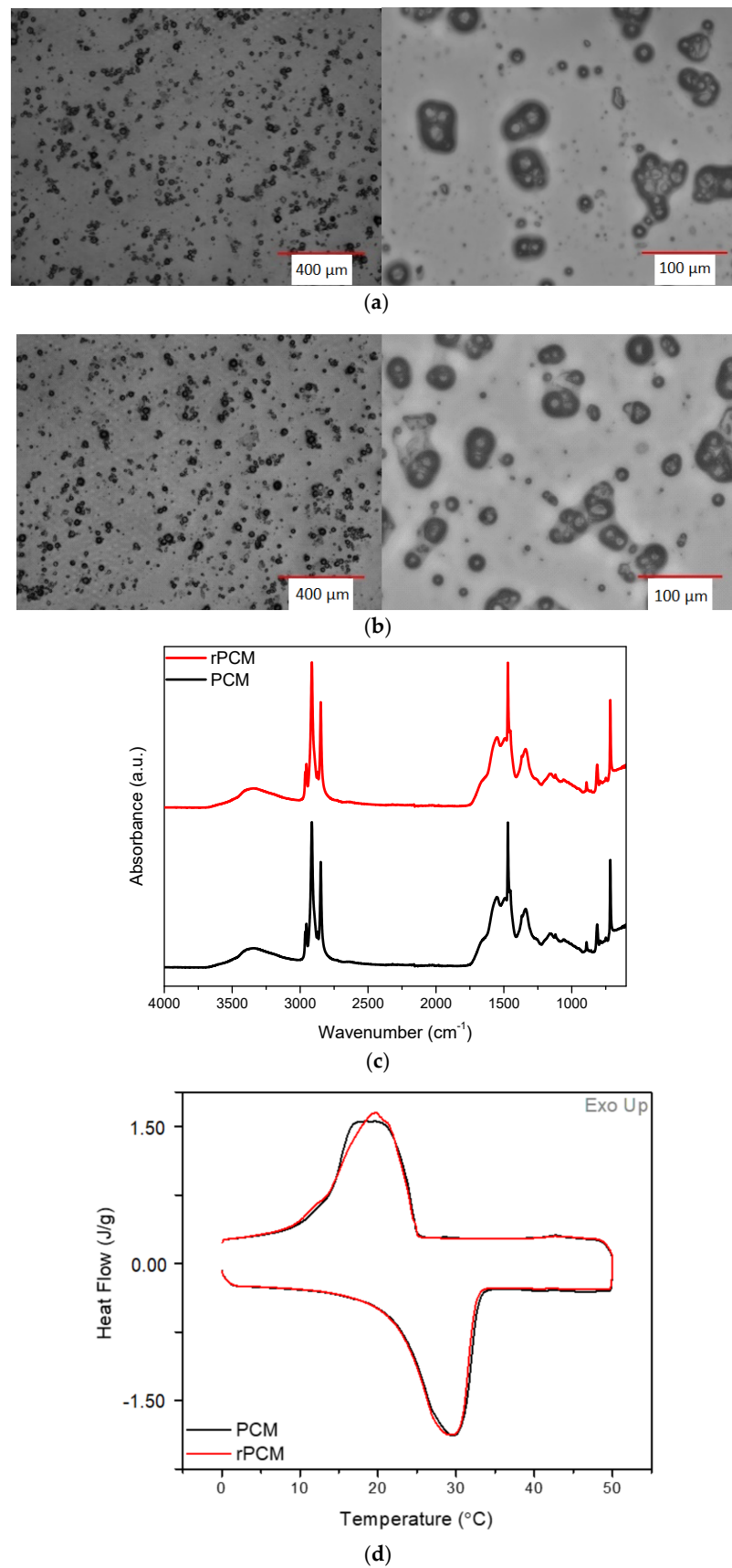


Figure 9. Optical microscope images of (a) original PCMs; (b) recovered PCMs; (c) FTIR spectra; (d) DSC thermograms of recovered PCM microcapsules in comparison to original PCM microcapsules.

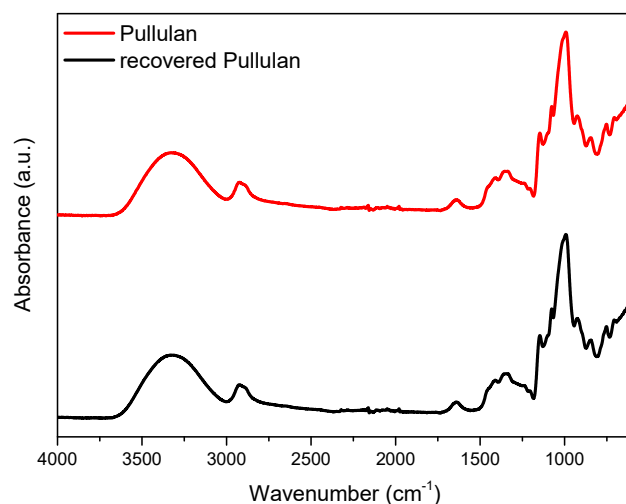


Figure 10. FTIR spectrum of recovered pullulan in comparison to fresh pullulan polymer.

4. Conclusions

Recyclable bio-based films with thermal management functionality using pullulan as the matrix polymer and Nextek 28D microcapsules as the PCM material were prepared. Uniform films with uniformly dispersed PCMs were obtained via the film-casting method. The composite films were white in colour. While neat pullulan films showed no phase transitions between 0 and 50 °C, pullulan-based composite films showed melting and crystallization due to the presence of encapsulated PCMs. While the phase transition temperatures of the films showed no apparent variations compared to that of PCMs, the enthalpy values of the bio-based films increased with the increase in the PCM content. The melting enthalpy increased from 21.94 to 104.85 J g⁻¹, and the crystallization enthalpy increased from 20.92 to 103.58 J g⁻¹ as the PCM content increased from 15 to 75 wt.%. The composite films prepared with 75 wt.% PCM incorporation exhibited 104.85 J g⁻¹ of enthalpy storage during heating with 80.7% efficiency. The crystallization enthalpy was 103.58 J g⁻¹ with an efficiency of 81%. Additionally, the application of thermal cycles indicated that the bio-based composite films showed good thermal reliability as their thermal properties were well retained after thermal cycling. The PCMs and pullulan polymer could be recovered with a yield of approximately 95% and 93% respectively. The morphology, chemical structure, and thermal properties of the PCMs were maintained after the recovery process, which showed the reusability of the PCMs. The chemical structure of the recovered pullulan was identical to that of the fresh pullulan polymer. The easily applicable bio-based composite films with thermal management functionality and recyclability appeared to provide an innovative system for packaging and storage applications.

Funding: This research received no external funding.

Institutional Review Board Statement: Not applicable.

Informed Consent Statement: Not applicable.

Data Availability Statement: The data presented in this study are available on request from the corresponding author.

Conflicts of Interest: The author declares no competing interest.

References

1. Kraśniewska, K.; Pobiega, K.; Gniewosz, M. Pullulan-Biopolymer with Potential for Use as Food Packaging. *Int. J. Food Eng.* **2019**, *15*, 20190030. [[CrossRef](#)]
2. Hassannia-Kolae, M.; Khodaiyan, F.; Pourahmad, R.; Shahabi-Ghahfarrokhi, I. Development of Ecofriendly Bionanocomposite: Whey Protein Isolate/Pullulan Films with Nano-SiO₂. *Int. J. Biol. Macromol.* **2016**, *86*, 139–144. [[CrossRef](#)]

3. Shahabi-Ghahfarrokhi, I.; Khodaiyan, F.; Mousavi, M.; Yousefi, H. Preparation of UV-Protective Kefiran/Nano-ZnO Nanocomposites: Physical and Mechanical Properties. *Int. J. Biol. Macromol.* **2015**, *72*, 41–46. [[CrossRef](#)]
4. Rhim, J.W.; Lee, S.B.; Hong, S.I. Preparation and Characterization of Agar/Clay Nanocomposite Films: The Effect of Clay Type. *J. Food Sci.* **2011**, *76*, N40–N48. [[CrossRef](#)] [[PubMed](#)]
5. Trovatti, E.; Fernandes, S.C.M.; Rubatat, L.; Perez, D.d.S.; Freire, C.S.R.; Silvestre, A.J.D.; Neto, C.P. Pullulan-Nanofibrillated Cellulose Composite Films with Improved Thermal and Mechanical Properties. *Compos. Sci. Technol.* **2012**, *72*, 1556–1561. [[CrossRef](#)]
6. Cozzolino, C.A.; Cerri, G.; Brundu, A.; Farris, S. Microfibrillated Cellulose (MFC): Pullulan Bionanocomposite Films. *Cellulose* **2014**, *21*, 4323–4335. [[CrossRef](#)]
7. Silva, N.H.C.S.; Vilela, C.; Almeida, A.; Marrucho, I.M.; Freire, C.S.R. Pullulan-Based Nanocomposite Films for Functional Food Packaging: Exploiting Lysozyme Nanofibers as Antibacterial and Antioxidant Reinforcing Additives. *Food Hydrocoll.* **2018**, *77*, 921–930. [[CrossRef](#)]
8. Introzzi, L.; Fuentes-Alventosa, J.J.; Cozzolino, C.A.; Trabattoni, S.; Tavazzi, S.; Bianchi, C.L.; Schiraldi, A.; Piergiovanni, L.; Farris, S. “Wetting Enhancer” Pullulan Coating for Antifog Packaging Applications. *ACS Appl. Mater. Interfaces* **2012**, *4*, 3692–3700. [[CrossRef](#)]
9. Hassannia-Kolae, M.; Khodaiyan, F.; Shahabi-Ghahfarrokhi, I. Modification of Functional Properties of Pullulan-Whey Protein Bionanocomposite Films with Nanoclay. *J. Food Sci. Technol.* **2016**, *53*, 1294–1302. [[CrossRef](#)]
10. Pinto, R.J.B.; Almeida, A.; Fernandes, S.C.M.; Freire, C.S.R.; Silvestre, A.J.D.; Neto, C.P.; Trindade, T. Antifungal Activity of Transparent Nanocomposite Thin Films of Pullulan and Silver against *Aspergillus Niger*. *Colloids Surf. B Biointerfaces* **2013**, *103*, 143–148. [[CrossRef](#)]
11. Liu, Y.; Liu, Y.; Han, K.; Cai, Y.; Ma, M.; Tong, Q.; Sheng, L. Effect of Nano-TiO₂ on the Physical, Mechanical and Optical Properties of Pullulan Film. *Carbohydr. Polym.* **2019**, *218*, 95–102. [[CrossRef](#)] [[PubMed](#)]
12. Ho, C.P.; Fan, J.; Newton, E.; Au, R. Improving Thermal Comfort in Apparel. In *Improving Comfort in Clothing*; Song, G., Ed.; Woodhead Publishing: Cambridge, UK, 2011; pp. 165–181. ISBN 978-1-84569-539-2.
13. Das, A.; Alagirusamy, R. Introduction to Clothing Comfort. In *Science in Clothing Comfort*; Das, A., Alagirusamy, R., Eds.; Woodhead Publishing India: New Delhi, India, 2010; pp. 1–12. ISBN 978-1-84569-789-1.
14. Erkan, G. Enhancing The Thermal Properties of Textiles With Phase Change Materials. *Res. J. Text. Appar.* **2004**, *8*, 57–64. [[CrossRef](#)]
15. Mondal, S. Phase Change Materials for Smart Textiles—An Overview. *Appl. Therm. Eng.* **2008**, *28*, 1536–1550. [[CrossRef](#)]
16. Sarier, N.; Onder, E. Organic Phase Change Materials and Their Textile Applications: An Overview. *Thermochim. Acta* **2012**, *540*, 7–60. [[CrossRef](#)]
17. Alay, S.; Alkan, C.; Göde, F. Synthesis and Characterization of Poly(Methyl Methacrylate)/n-Hexadecane Microcapsules Using Different Cross-Linkers and Their Application to Some Fabrics. *Thermochim. Acta* **2011**, *518*, 1–8. [[CrossRef](#)]
18. Nelson, G. Application of Microencapsulation in Textiles. *Int. J. Pharm.* **2002**, *242*, 55–62. [[CrossRef](#)] [[PubMed](#)]
19. Sarier, N.; Onder, E. The Manufacture of Microencapsulated Phase Change Materials Suitable for the Design of Thermally Enhanced Fabrics. *Thermochim. Acta* **2007**, *452*, 149–160. [[CrossRef](#)]
20. Zhang, W.; Hao, S.; Zhao, D.; Bai, G.; Zuo, X.; Yao, J. Preparation of PMMA/SiO₂ PCM Microcapsules and Its Thermal Regulation Performance on Denim Fabric. *Pigment Resin Technol.* **2020**, *49*, 491–499. [[CrossRef](#)]
21. Marani, A.; Nehdi, M.L. Integrating Phase Change Materials in Construction Materials: Critical Review. *Constr. Build. Mater.* **2019**, *217*, 36–49. [[CrossRef](#)]
22. Mohaisen, K.O.; Hasan Zahir, M.; Maslehuddin, M.; Al-Dulaijan, S.U. Development of a Shape-Stabilized Phase Change Material Utilizing Natural and Industrial Byproducts for Thermal Energy Storage in Buildings. *J. Energy Storage* **2022**, *50*, 104205. [[CrossRef](#)]
23. Liu, H.; Wang, X.; Wu, D.; Ji, S. Fabrication and Applications of Dual-Responsive Microencapsulated Phase Change Material with Enhanced Solar Energy-Storage and Solar Photocatalytic Effectiveness. *Sol. Energy Mater. Sol. Cells* **2019**, *193*, 184–197. [[CrossRef](#)]
24. Choubineh, N.; Jannesari, H.; Kasaeian, A. Experimental Study of the Effect of Using Phase Change Materials on the Performance of an Air-Cooled Photovoltaic System. *Renew. Sustain. Energy Rev.* **2019**, *101*, 103–111. [[CrossRef](#)]
25. Mondieig, D.; Rajabalee, F.; Laprie, A.; Oonk, H.A.J.; Calvet, T.; Cuevas-Diarte, M.A. Protection of Temperature Sensitive Biomedical Products Using Molecular Alloys as Phase Change Material. *Transfus. Apher. Sci.* **2003**, *28*, 143–148. [[CrossRef](#)] [[PubMed](#)]
26. Kandasamy, R.; Wang, X.Q.; Mujumdar, A.S. Application of Phase Change Materials in Thermal Management of Electronics. *Appl. Therm. Eng.* **2007**, *27*, 2822–2832. [[CrossRef](#)]
27. Singh, S.; Gaikwad, K.; Youn, S.L. Phase Change Materials for Advanced Cooling Packaging. *Environ. Chem. Lett.* **2018**, *16*, 845–859. [[CrossRef](#)]
28. Gong, J.; Tang, W.; Xia, L.; Fu, Z.; Zhou, S.; Zhang, J.; Zhang, C.; Hua Ji, L.L.; Xu, W. Flexible and weavable 3D porous graphene/PPy/lignocellulose-based versatile fibrous wearables for thermal management and strain sensing. *Chem. Eng. J.* **2023**, *452*, 139338. [[CrossRef](#)]
29. Xiang, B.; Zhang, R.; Zeng, X.; Yanlong, L.; Zhenyang, L. An Easy-to-Prepare Flexible Dual-Mode Fiber Membrane for Daytime Outdoor Thermal Management. *Adv. Fiber Mater.* **2022**, *4*, 1058–1068. [[CrossRef](#)]
30. Pan, S.; Zhu, M. Nanoprocessed Silk Makes Skin Feel Cool. *Adv. Fiber Mater.* **2022**, *4*, 319–320. [[CrossRef](#)]

31. Choudhury, A.R.; Saluja, P.; Prasad, G.S. Pullulan Production by an Osmotolerant *Aureobasidium Pullulans* RBF-4A3 Isolated from Flowers of *Caesulia Axillaris*. *Carbohydr. Polym.* **2011**, *83*, 1547–1552. [[CrossRef](#)]
32. Terán Hilares, R.; Orsi, C.A.; Ahmed, M.A.; Marcelino, P.F.; Menegatti, C.R.; da Silva, S.S.; dos Santos, J.C. Low-Melanin Containing Pullulan Production from Sugarcane Bagasse Hydrolysate by *Aureobasidium Pullulans* in Fermentations Assisted by Light-Emitting Diode. *Bioresour. Technol.* **2017**, *230*, 76–81. [[CrossRef](#)]
33. Hamidi, M.; Kennedy, J.F.; Khodaiyan, F.; Mousavi, Z.; Hosseini, S.S. Production Optimization, Characterization and Gene Expression of Pullulan from a New Strain of *Aureobasidium Pullulans*. *Int. J. Biol. Macromol.* **2019**, *138*, 725–735. [[CrossRef](#)] [[PubMed](#)]
34. Li, Q.M.; Wang, J.F.; Zha, X.Q.; Pan, L.H.; Zhang, H.L.; Luo, J.P. Structural Characterization and Immunomodulatory Activity of a New Polysaccharide from Jellyfish. *Carbohydr. Polym.* **2017**, *159*, 188–194. [[CrossRef](#)] [[PubMed](#)]
35. Wu, J.; Zhong, F.; Li, Y.; Shoemaker, C.F.; Xia, W. Preparation and Characterization of Pullulan-Chitosan and Pullulan-Carboxymethyl Chitosan Blended Films. *Food Hydrocoll.* **2013**, *30*, 82–91. [[CrossRef](#)]
36. Niu, B.; Shao, P.; Chen, H.; Sun, P. Structural and Physicochemical Characterization of Novel Hydrophobic Packaging Films Based on Pullulan Derivatives for Fruits Preservation. *Carbohydr. Polym.* **2019**, *208*, 276–284. [[CrossRef](#)]
37. Cheng, K.-C.; Demirci, A.; Catchmark, J.M. Effects of Plastic Composite Support and PH Profiles on Pullulan Production in a Biofilm Reactor. *Appl. Microbiol. Biotechnol.* **2010**, *86*, 853–861. [[CrossRef](#)] [[PubMed](#)]
38. Trovatti, E.; Fernandes, S.C.M.; Rubatat, L.; Freire, C.S.R.; Silvestre, A.J.D.; Carlos, P.N. Sustainable Nanocomposite Films Based on Bacterial Cellulose and Pullulan. *Cellulose* **2012**, *19*, 729–737. [[CrossRef](#)]
39. Kumar, V.; Mirzaei, A.; Bonyani, M.; Kim, K.-H.; Kim, H.W.; Kim, S.S. Advances in Electrospun Nanofiber Fabrication for Polyaniline (PANI)-Based Chemoresistive Sensors for Gaseous Ammonia. *TRAC Trends Anal. Chem.* **2020**, *129*, 115938. [[CrossRef](#)]
40. Mirzaee, H.; Khodaiyan, F.; Kennedy, J.F.; Hosseini, S.S. Production, Optimization and Characterization of Pullulan from Sesame Seed Oil Cake as a New Substrate by *Aureobasidium Pullulans*. *Carbohydr. Polym. Technol. Appl.* **2020**, *1*, 100004. [[CrossRef](#)]
41. Liang, R.; Hu, A.; Hatat-Fraile, M.; Zhou, N. Fundamentals on Adsorption, Membrane Filtration, and Advanced Oxidation Processes for Water Treatment. In *Nanotechnology for Water Treatment and Purification*; Hu, A., Apblett, A., Eds.; Springer: Cham, Switzerland, 2014; Volume 22, pp. 1–45. ISBN 978-3-319-06577-9. [[CrossRef](#)]
42. Weiss, S.; Urdl, K.; Mayer, H.A.; Zikulnig-Rusch, E.M.; Kandelbauer, A. IR Spectroscopy: Suitable Method for Determination of Curing Degree and Crosslinking Type in Melamine-Formaldehyde Resins. *J. Appl. Polym. Sci.* **2019**, *136*, 47691. [[CrossRef](#)]
43. Krupa, I.; Nógellová, Z.; Špitalský, Z.; Janigová, I.; Boh, B.; Sumiga, B.; Kleinová, A.; Karkri, M.; Almaadeed, M.A. Phase Change Materials Based on High-Density Polyethylene Filled with Microencapsulated Paraffin Wax. *Energy Convers. Manag.* **2014**, *87*, 400–409. [[CrossRef](#)]
44. Kizildag, N. Smart Composite Nanofiber Mats with Thermal Management Functionality. *Sci. Rep.* **2021**, *11*, 4256. [[CrossRef](#)] [[PubMed](#)]
45. He, Y.; Li, H.; Luo, F.; Jin, Y.; Huang, B.; Qingrong, Q. Bio-based flexible phase change composite film with high thermal conductivity for thermal energy storage Composites Part A. *Appl. Sci. Manuf.* **2021**, *151*, 106638. [[CrossRef](#)]

Disclaimer/Publisher's Note: The statements, opinions and data contained in all publications are solely those of the individual author(s) and contributor(s) and not of MDPI and/or the editor(s). MDPI and/or the editor(s) disclaim responsibility for any injury to people or property resulting from any ideas, methods, instructions or products referred to in the content.